applied sciences

MDPI

Article

Force and Sound Pressure Sensors Used for Modeling the Impact of the Firearm with a Suppressor

Jaroslaw Selech [1], Artūras Kilikevičius [2], Kristina Kilikevičienė [3], Sergejus Borodinas [4], Jonas Matijošius [2,*], Darius Vainorius [2], Jacek Marcinkiewicz [1] and Zaneta Staszak [1]

1 The Faculty of Civil and Transport Engineering, Poznan University of Technology, 5 M. Skłodowska-Curie Square PL-60-965 Poznan, Poland; jaroslaw.selech@put.poznan.pl (J.S.); jacek.marcinkiewicz@put.poznan.pl (J.M.); zaneta.staszak@put.poznan.pl (Z.S.)

2 Institute of Mechanical Science, Vilnius Gediminas Technical University, J. Basanavičiaus str. 28, LT-03224 Vilnius, Lithuania; arturas.kilikevicius@vgtu.lt (A.K.); darius.vainorius@vgtu.lt (D.V.)

3 Department of Mechanical and Material Engineering, Vilnius Gediminas Technical University, J. Basanavičiaus str. 28, LT-03224 Vilnius, Lithuania; kristina.kilikeviciene@vgtu.lt

4 Department of Applied Mechanics, Vilnius Gediminas Technical University, Saulėtekio av. 11, 10223 Vilnius, Lithuania; sergejus.borodinas@vgtu.lt

* Correspondence: jonas.matijosius@vgtu.lt; Tel.: +370-684-04-169

Received: 23 December 2019; Accepted: 30 January 2020; Published: 2 February 2020

Abstract: In this paper, a mathematical model for projectiles shooting in any direction based on sensors distributed stereoscopically is put forward. It is based on the characteristics of a shock wave around a supersonic projectile and acoustical localization. Wave equations for an acoustic monopole point source of a directed effect used for physical interpretation of pressure as an acoustic phenomenon. Simulation and measurements of novel versatile mechanical and acoustical damping system (silencer), which has both a muzzle break and silencer properties studied in this paper. The use of the proposed damping system can have great influence on the acoustic pressure field intensity from the shooter. A silencer regarded as an acoustic transducer and multi-holes waveguide with a chamber. Wave equations for an acoustic monopole point source of a directed effect used for the physical interpretation of pressure as an acoustic phenomenon. The numerical simulation results of the silencer with different configurations presented allow trends to be established. A measurement chain was used to compare the simulation results with the experimental ones. The modeling and experimental results showed an increase in silencer chamber volume results in a reduction of recorded pressure within the silencer chamber.

Keywords: force sensor; silencer; point wave source; dynamic impact; sound pressure

1. Introduction

The results of acoustic and force sensors' measurement and their use in shooting simulation are analyzed in a series of articles. Acoustic parameters and force measurement technology is widely used in the assessment of the characteristics of the shot. Parameters of firearms and their accessories (sights, silencer, etc.) are research objects of many studies worldwide, as the high precision and reliability of their evaluation is required by state authorities of weapon supervision. A modern silencer of the firearm is vastly superior to ear-level protection and the only available form of suppression capable of making certain sporting arms safe for hearing [1–8]. Forces show an increasing number of cases of hearing damage [9–15]. Many of the early developments of the silencer were mainly empirical in nature [16–25].

The basic purpose of the silencer is to mask the position of the weapon, which can be precisely determined similarly to locating the blasting source [26–31]. A silencer suppresses the firing sound in

several ways: by reducing the inner energy of the powder gases coming out of the barrel, by reducing their output velocity and temperature, or by breaking the powder gas flow and by making it whirl. All firearm silencers offered significantly greater noise reduction than ear-level protection, which is usually greater than 50%. Noise reduction of all ear-level protectors is unable to reduce the impulse pressure below 140 dB for certain common firearms.

The firing sound is a combination of a number of acoustic waves formed as a result of four main components: the gunpowder gas flow muzzle wave, the shock wave generated due to the supersonic projectile movement, the wave formed by the air column ejected from the gun barrel in front of the projectile, and the acoustic wave generated by collision of gun parts during the firing process.

The US Army's Ballistic Research Laboratory (BRL) has developed a prediction method for muzzle devices [32] based on gathered experimental data on muzzle devices for distances from 10 to 50 calibers from the muzzle [33–35]. Helliker and other scientists [16,27,36–42] investigated many different muzzle devices including a silencer. The outputs of the models were not verified against experimental test data from muzzle blasts, which differ to conventional blast waves [43–48].

Carson and Sahni [49] studied containment devices in more detail both theoretically and experimentally in three approaches: acoustic theory, blast theory, and quasi-one-dimensional flow theory.

Blast attenuation increased rapidly with the number of baffles in a silencer before maximum attenuation was achieved and a gradual decline occurred [50–56].

It is well known that, while the projectile accelerates with a high temperature and high pressure, the explosion of propellant gases generates the muzzle blast wave [49,57–65]. Since the muzzle energy increases, the impulsive wave intensity is estimated accordingly. A shot, as an impulse shock wave coming from the weapon, has many negative effects on people and the environment. Unlike other sounds, shock wave has high energy, low frequency, and impulsiveness. It is strongly directed and has long-range propagation [66–74]. The muzzle blast is strongly directed.

Kirby [75] noted that both the Boundary Element Method and Finite Element Analysis have been used as tools to model the gas flows in vehicle exhaust silencers.

Cummings [36] suggests that computational methods require considerable effort and can be difficult to track and other mathematical models are also reliant on very low Mach number velocities, which limits their application within firearms.

In this paper, authors used the acoustic-solid interaction COMSOL multi-physics interface for finding a solid domain reaction (barrel with/without silencer) to the acoustic explosion inside the barrel, which corresponds to the blasting effect [76].

The main advantage of this device is that the sound is suppressed mainly in the area of the shooter while, in the direction of the shot, the sound is suppressed by up to 30% (and this device does not belong to the mufflers) and can, therefore, be used in hunting because if, in the direction of the shot, sound is suppressed by more than 30%, hunting would not be possible. Thus, a blocking device imposed for use in hunting has been developed and its use significantly reduces the sound pressure in the shooter zone and, in addition, significantly reduces the kickback force.

The newly developed suppression device is intended for use in the leisure and non-military industry. The newly developed silencer would be a mixture of the silencer and muzzle brake designed to reduce noise and kickback. The main advantage of this unit is that the sound is suppressed mainly in the shooter area and up to 30% in the firing direction (and this indicator does not count as suppressors). As a result, the damping device can be used in leisure activities, as if the sound was suppressed by more than 30% in the direction of the firing. The damping device would be classified as dampers, which are not legal in many European countries like Lithuania.

The silencer muzzle brake is widely described in both scientific and patent materials. However, there is hardly any information on devices with the desired damping-braking properties. This type of device is not for sale.

The silencer and muzzle brake problems are most often addressed in the scientific literature: impact on bullet trajectory [77–79], effects of sound pressure generated during the shot on hearing [80–85], and reducing the sound pressure of firearms by using various types of silencers [86–88]. However, problems related to the use of the device for recreational use are not addressed.

A prototype is currently being developed at JSC Oksalis, and the determination of the properties (acoustic parameters and kickback force) of this prototype would allow for a well-validated theoretical model based on the results obtained. With the right model and theoretical optimization studies, it would be possible to retest and evaluate the performance of the damping-braking device. The goal is to achieve optimum damping-braking device characteristics and to evaluate the production capabilities.

2. Materials and Methods

The object of the investigation is a damping system used in a firearm. Explosive Weapon (Merkel RX Helix Black 308 Win) is presented in Figure 1a. The damping system is shown in Figure 1a–c, respectively. Images of a suppression system fitted to the weapon are shown in Figure 1a,c. Assembly of the damping system (silencer) is presented in Figure 1b.

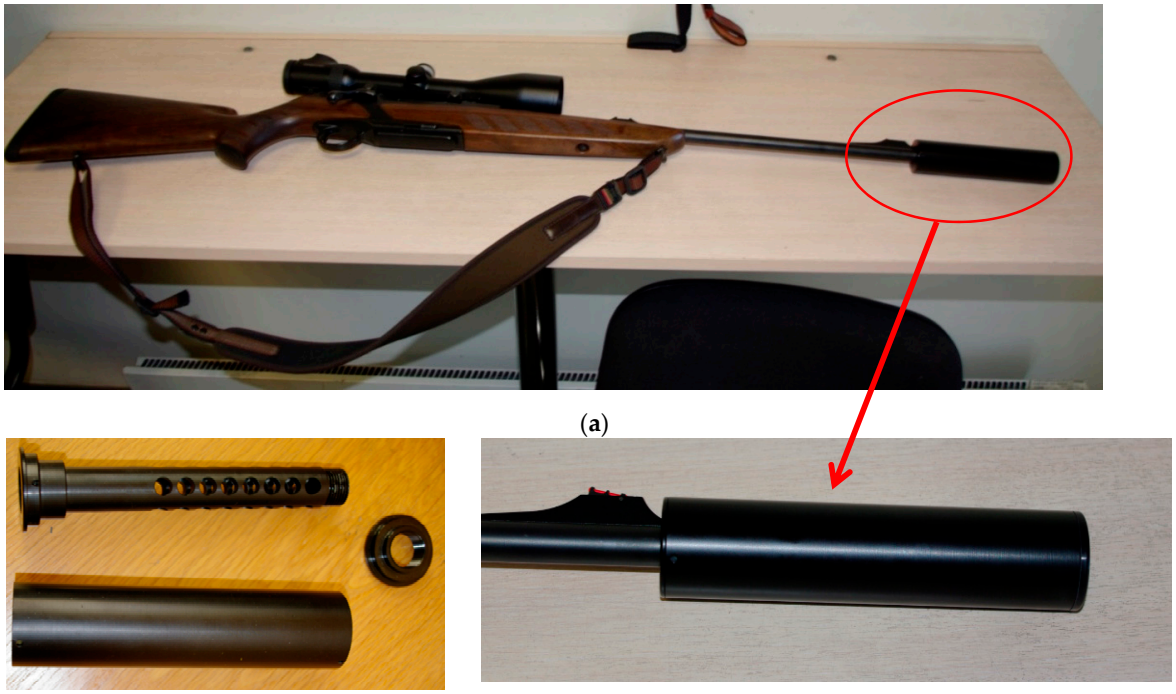

Figure 1. Firearm with a fire damping system (silencer): (**a**) explosive weapon (Merkel RX Helix Black 308 Win); (**b**) assembly of the damping system (silencer); (**c**) a suppression system fitted to the weapon.

In the design process, computational simulations are used to investigate how different geometries and operational parameters affect optimizing the performance of systems (Figure 2). Of the available computational tools, COMSOL Multiphysics applies a finite element method to solve different physics and engineering problems (e.g., acoustic propagation) governed by partial differential equations (PDEs). The acoustic-solid interaction, transient multi-physics interface combines the pressure acoustics as well as transient and solid mechanics interfaces to connect the acoustic pressure variations in the air domain to the structural deformation in the solid domain. A dedicated multi-physics coupling condition is readily defined for the air-solid boundary and sets up the air loads on the solid domain and the effect of the structural accelerations on the air. Each module is governed by its own equations that describe the specific physics.

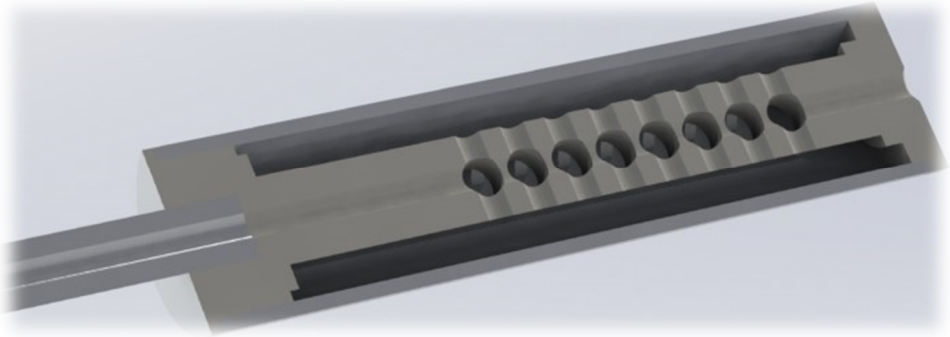

Figure 2. CAD assembly of 3D silencer model section view included chamber and internal holes.

The pressure acoustics model involves a monopole point source that considers the flow pulse at the center of a barrel bottom (Figure 3) to illustrate some properties of time-dependent acoustic problems [89]. The acoustic pressure field $p(x,t)$, along the barrel is given by the scalar wave equation shown below.

$$\frac{1}{\rho c^2}\frac{\partial^2 p}{\partial t^2} + \nabla\cdot\left(-\frac{1}{\rho}(\nabla p_t - q_d)\right) = S(x,t), \quad (1)$$

where p_t is the total acoustic pressure, ρ is air density, c is speed of sound, and q_d is the dipole domain source, which represents a domain volumetric force and $S(x,t)$ is the monopole point source term given by the equation below.

$$S(x,t) = \frac{4\pi}{\rho_c} S\delta(x - x_0), \quad (2)$$

where $\delta(x - x_0)$ is the delta function in three dimensions and adds the source at the point where $x = x_0$.

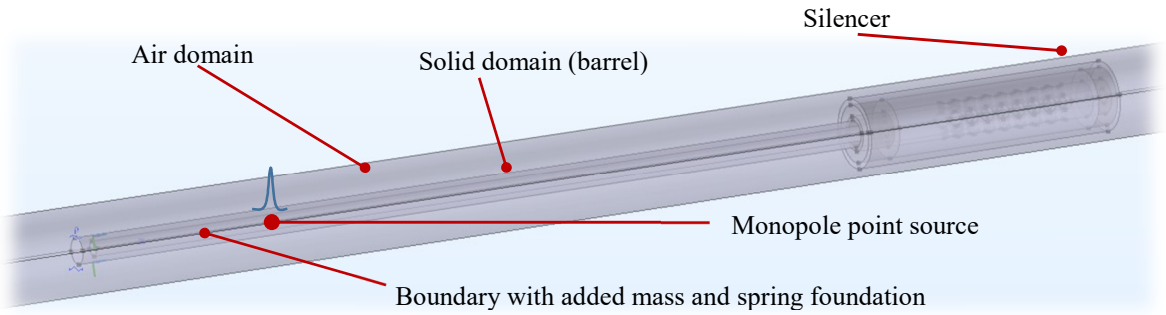

Figure 3. CAD assembly of the 3D silencer with barrel and some boundary condition.

The monopole amplitude S depends on the source type and, in our calculation, is the volume flow rate out from the source (peak 4 m^3/s). All external boundaries of the air domain are established as a spherical wave radiation. This radiation condition allows an outgoing spherical wave to leave the modeling air domain with minimal reflections. The maximum element size is closely related to the speed of sound in the air, frequency bandwidth, and number of elements per wavelength (we used N = 4).

In the pressure acoustics and solid mechanics model simulation, several assumptions were made: (1) only isotropic loss factor of the mechanical system is taken into account, (2) the monopole point source time duration is about 1, 2 ms (in real rifle barrel, the shot duration vary from 1 to 60 ms), (3) the holes number of the silencer are selected from 7 to 9 and used in a parametric sweep of the time-dependent study, and (4) the monopole point source has a normal distribution waveform of flow pulse in modeling. The default temperature and initial pressure estimated 20 °C and 0 Pa, respectively. Moreover, the bottom of a barrel has 90 kg of added mass and a spring foundation, as shown in Figure 3.

During the research, the dynamic effects of a bullet caused by a silencer are examined. The study used a bullet (180 g).

The main object of current research in this paper is the silencer's design. According to the technical requirements, the sound level pressure field and rifle delivery will be minimized from the shooting side, but the sound level pressure from the target is not necessary to attenuation.

Brüel & Kjær measuring instruments were used to measure force and sound pressure parameters. The mobile measurement results processing equipment "3660-D" with DELL computers (Figure 4c). The force sensor 8320-002 (Figure 4a) were mounted on the gun backrest. The apparatus for measuring the sound pressure is shown in Figure 4d. This part depicts an audio analyzer with a microphone 2250 and a hydrophone 8103 [90,91].

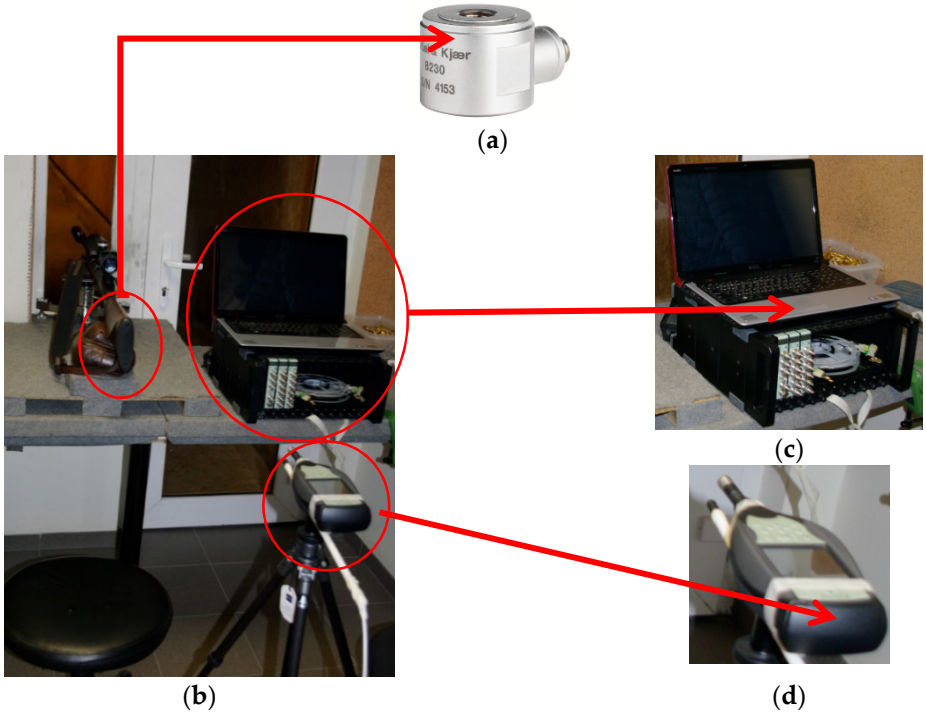

Figure 4. Experimental setup for force and sound pressure measurements: (**a**) the force sensor 8320-002; (**b**) the testing bench; (**c**) the mobile measurement results processing equipment "3660-D" with DELL computers; (**d**) the apparatus for measuring the sound pressure (Hydrophone 8103).

The received measurement signals from the computer were processed using static data processing package Origin 6 and Pulse software packages. Signal spectra, distributions, and statistical parameters were calculated.

Arithmetic mean:

$$\overline{x} = \frac{1}{n}\sum_{i=1}^{n} x_i, \tag{3}$$

Standard deviation:

$$S_X = \sqrt{\frac{1}{n-1}\sum_{i=1}^{n}(x_i - \overline{x})^2}, \tag{4}$$

where n—the number of measurement results. x_i—the ith measurement result.

3. Results

3.1. Measurements Results of the Firearm's Backrest Force

Measurements of the firearm's backrest force were carried out using a force-measuring device (Figure 4a).

During the study, the dynamic effects caused by a different bullet on a rifle were examined. The typical graphs of the backrest forces in the end of the rifle's back (Figure 4a) are shown in Figure 5. The statistical parameters of the results are presented in Table 1.

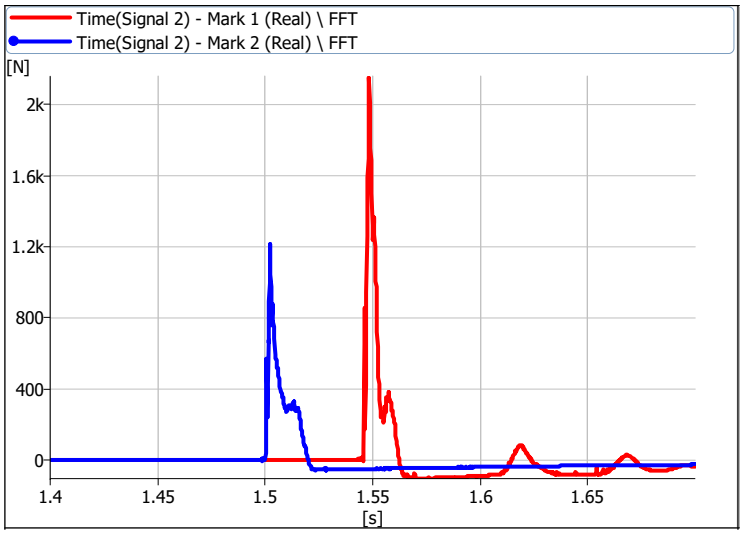

Figure 5. Typical time alteration graphs representing generated forces of the reaper of the rear barrel directed at a human. Blue—when the silencer is used. Red—when the silencer is not used.

Table 1. Statistical characteristics of force measurement results.

Setup *	**Force, N**			
	Mean	Standard Deviation	Minimum	Maximum
A	1195.667	10.841	1173	1214
B	2192.333	4.5056	2185	2200

* A—with silencer. B—without silencer.

The statistical characteristics of the results of the measurement of force in Table 1 show that the damper reduces the force from 2,192,333 to 1,195,667 N. Therefore, it can be seen that the damping device significantly reduces the amount of force directed at the person, which is obtained during the shooting.

The formula used to evaluate the damping force is shown below.

$$T_N = (1 - F_{\text{with silencer}}/F_{\text{without silencer}}) * 100\%. \quad (5)$$

The damping evaluating the magnitude of force is given below.

$$T_N = (1 - F_{\text{with silencer}}/F_{\text{without silencer}}) * 100\% = (1 - 1195.667/2192.333) * 100\% = 45.46\%$$

The results show that the damping device significantly reduces the amount of force directed at a person (reduction of 45.46%).

3.2. Sound Pressure Measurement Results

Sound pressure measurements were carried out using the hydrophone 8103. Sound pressure (Figure 4d), when the shot is being made, the time of change, and the spectral density graphs when shooting with and without the silencer is shown in Figure 6. The statistical parameters of the test are presented in Table 2 as well.

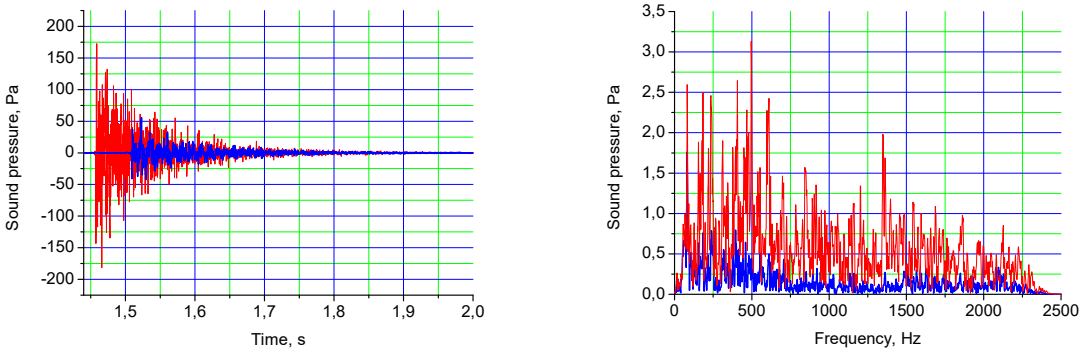

(**a**) (**b**)

Figure 6. Typical sound pressure graphs: (**a**) a time alteration (**b**) a spectral density, when a shot with a barrel is performed. Blue—when the silencer is used. Red—when the silencer is not used.

Table 2. Statistical characteristics of sound pressure measurement results.

Setup *	**Sound Pressure, Pa**			
	Mean	Standard Deviation	Minimum	Maximum
A	92.517	1.505	91.3	94.2
B	350.767	3.287	347.8	354.3

* A—with silencer. B—without silencer.

The statistical characteristics of the sound pressure measurement results in Table 2 show that the damping device (silencer) reduces the sound pressure from 350.767 to 92.517 Pa. Thus, it can be seen that the silencer significantly reduces the sound pressure obtained during the shooting.

The sound pressure damping in relation to the pressure level is given below.

$$T_P = (1 - (P_{\text{with silencer max}} + |P_{\text{with silencer min}}|)/(P_{\text{without silencer max}} + |P_{\text{without silencer min}}|)) * 100\%. \quad (6)$$

Damping evaluating the pressure level is given below.

$$T_{P\ \text{pressure Vulkan}} = (1 - (P_{\text{with silencer max}} + |P_{\text{with silencer min}}|)/(P_{\text{without silencer max}} + |P_{\text{without silencer min}}|)) * 100\% = (1 - 92.517/350.767) * 100\% = 73.6\%. \quad (7)$$

The 73.6% reduction in sound pressure achieved with the use of an additional silencer during firing suggests that the silencer used during firing significantly increases the sound pressure in the shooter area.

4. Discussion

Figures 7 and 8 show the backrest's (Figure 4) rear part. When the shot is executed, the forces are directed to human time and spectral density graphs during the shooting as well as when a damper is used and not used.

The instantaneous local acceleration in the air domain's point is reflected to the sound pressure level (SPL). Time-dependent numerical simulation results in the local point of the barrel bottom is

shown in Figure 7a. In four cases, only a barrel without the silencer and with 7–9 hole silencer types. A normalized characteristic of local acceleration in the point of the air domain 1 m distance from the bottom of the barrel in the first 10 periods of the shot are degreased using the silencer (all colors instead of the dark blue in Figure 7a). We can assume that the acoustic sound pressure from this side is also degreasing when compared with the calculation of a standard rifle barrel (dark blue line in Figure 7a). The acceleration in the far-field degrease faster using a silencer on the barrel exit.

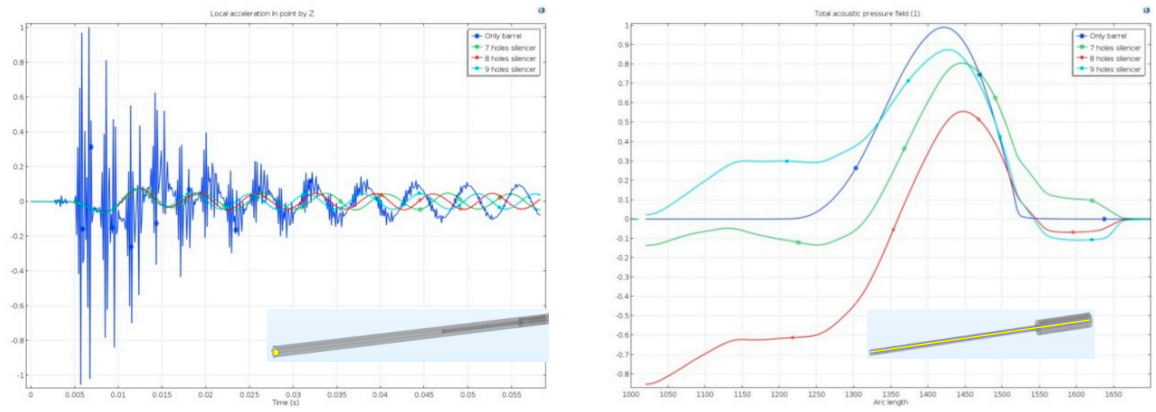

(**a**) (**b**)

Figure 7. Normalized local acceleration in the point 1 m from the barrel bottom by Z-axes (**a**) and total acoustic pressure field along the yellow line inside the barrel (**b**): dark blue—only barrel, other colors—with a 7–9-holes silencer.

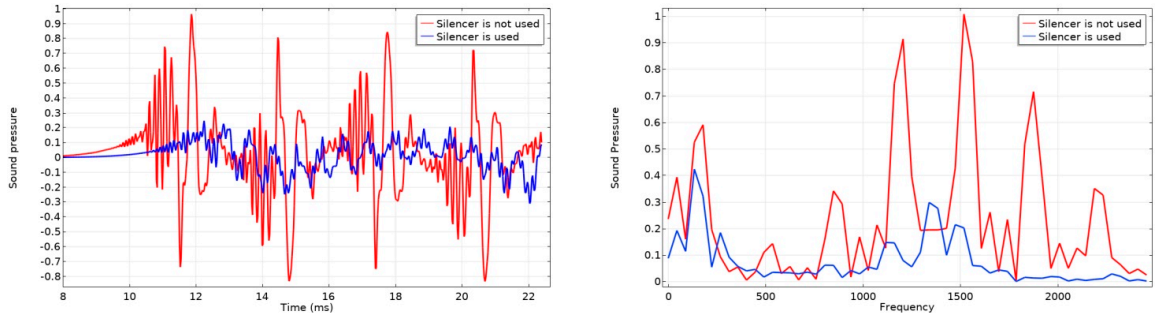

(**a**) (**b**)

Figure 8. Normalized sound pressure in the point 1 m from the barrel bottom: (time alteration (**a**) and spectral density (**b**)) when a shot with a barrel is performed. Blue—when the silencer is used. Red—when the silencer is not used.

Total acoustic pressure field along the barrel (yellow line) is shown in Figure 7b. According to the numerical calculation and the pressure field inside the barrel, using the 8holes silencer type degreased almost twice.

Normalized sound pressure in the point 1 m from the barrel bottom in the time domain with and without the silencer is shown in Figure 8a. Good enough acoustical damping performance is represented using an 8-holes silencer. Another characteristic of analyzing vibration data is in the frequency domain, which is the most vibration analyzing type. Using a spectrogram, we get a much deeper understanding of the vibration profile and how it changes with time. The FFT (fast Fourier transform) takes a block of time-domain data (Figure 8a) and returns the frequency spectrum of the data (Figure 8b). The main data presents the highest harmonics are attenuated by the silencer. Low frequency harmonics has a lower amplitude (blue line in Figure 8b).

The SPL distribution on the frequency of 10 Hz both for the system when the silencer is not used and used is shown in Figure 9. We can see than SPL from the "man" view is reduced (Figure 9b) when compared with the initial (standard) system (Figure 9a). Another very famous and useful acoustic field is the polar plot diagram, which represents the SPL distribution of the exterior-field, based on far-field integral calculation on the air surface in a pressure acoustics model. Two polar plot diagrams for frequencies 110 Hz and 1100 Hz are presented in Figure 10a,b, respectively. We can assume that, using the silencer, we can reduce or slightly control SPLs that depend on our requirements.

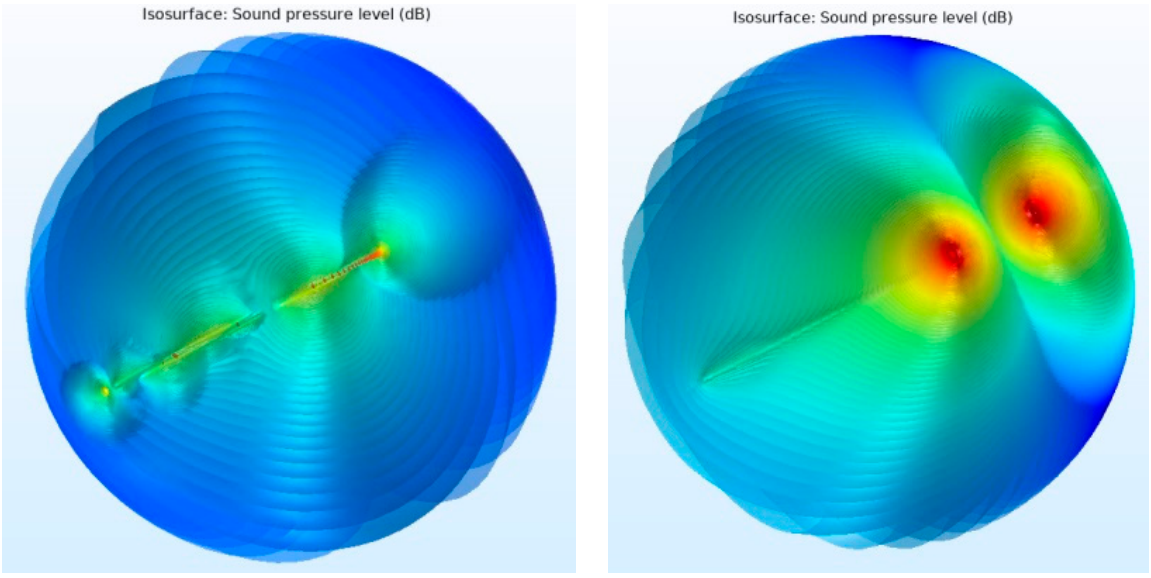

(**a**) (**b**)

Figure 9. (SPL) (10 Hz) iso-surface of the initial system (**a**) and system with a silencer (**b**).

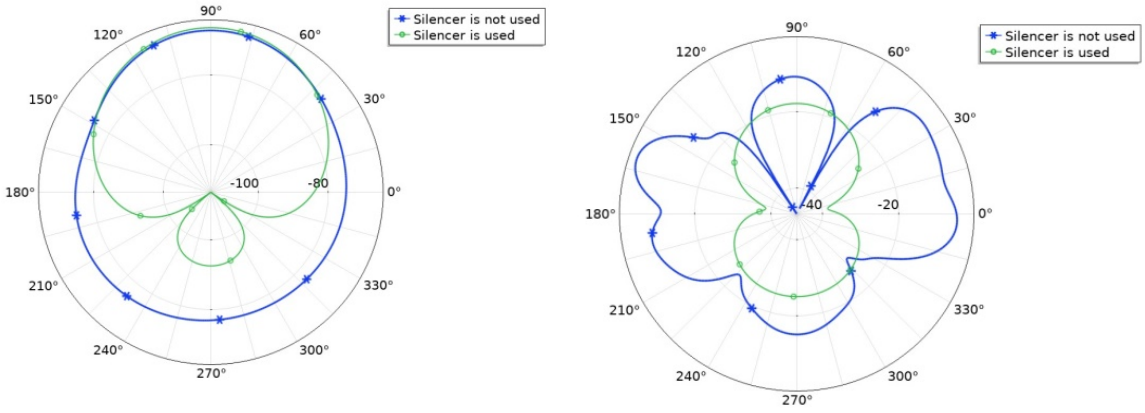

(**a**) (**b**)

Figure 10. Exterior-field SPL (far-field)—110 Hz (**a**) and 1100 Hz (**b**).

Studies carried out to analyze the barrel of different characteristics show that the pressure is reduced in part of the damper where the cavities are made. The pressure drop does not exceed 15%. Airflow simulations have shown that the airflow rate at the exit increased by 8%. In assessing these results, it can be assumed that this system directs the flow along the shot and, thereby, suppresses the acoustic sound pressure (noise) in the fire zone.

5. Conclusions

The research shows that, using force and sound pressure sensor measurement results of modeling, can be accurately determined by modeling the impact of the muzzle brake to acoustic and force parameters.

The research examined the effect of the newly created damper on the dynamic parameters during the shooting.

The results show that the damping device significantly reduces the rebound force of a gun directed to a person, which appears during the shot. The force is caused by the use of a damper that decreases by 45.46%.

The results show that the silencer significantly reduces the value of the sound pressure in the shooter zone during the shooting. The amount of the sound pressure value caused by the firing in the shooter area decreases by 73.6% using the additional silencer.

According to the technical requirements, the sound level pressure field and rifle delivery will be minimized from the shooting side. According to a numerical calculation, the pressure field inside the barrel, using the 8-holes silencer type, degreased almost twice.

Author Contributions: Conceptualization, J.S., K.K., and J.M. (Jonas Matijošius). Methodology, A.K. and J.M. (Jacek Marcinkiewicz). Software, S.B. and Z.S. Validation, J.S. and J.M. (Jacek Marcinkiewicz). Formal analysis, K.K. and Z.S. Investigation, J.M. (Jonas Matijošius). Resources, A.K. Data curation, S.B. and D.V. Writing—original draft preparation, J.S., A.K., and J.M. (Jonas Matijošius). Writing—review and editing, A.K. Visualization, K.K. and D.V. Supervision, S.B. Project administration, J.M. (Jonas Matijošius). All authors have read and agreed to the published version of the manuscript.

Funding: This research received no external funding.

Conflicts of Interest: The authors declare no conflict of interest.

References

1. Branch, M.P. Comparison of Muzzle Suppression and Ear-Level Hearing Protection in Firearm Use. *Otolaryngol. Head Neck Surg.* **2011**, *144*, 950–953. [CrossRef] [PubMed]
2. Arslan, H.; Ranjbar, M.; Secgin, E.; Celik, V. Theoretical and experimental investigation of acoustic performance of multi-chamber reactive silencers. *Appl. Acoust.* **2020**, *157*, 106987. [CrossRef]
3. Strong, B.L.; Ballard, S.-B.; Braund, W. The American College of Preventive Medicine Policy Recommendations on Reducing and Preventing Firearm-Related Injuries and Deaths. *Am. J. Prev. Med.* **2016**, *51*, 1084–1089. [CrossRef] [PubMed]
4. Itabashi, H.H.; Andrews, J.M.; Tomiyasu, U.; Erlich, S.S.; Sathyavagiswaran, L. Injuries due to firearms and other missile-launching devices. In *Forensic Neuropathology*; Elsevier: Amsterdam, The Netherlands, 2007; pp. 211–254, ISBN 978-0-12-058527-4.
5. Hamilton, D.; Lemeshow, S.; Saleska, J.L.; Brewer, B.; Strobino, K. Who owns guns and how do they keep them? The influence of household characteristics on firearms ownership and storage practices in the United States. *Prev. Med.* **2018**, *116*, 134–142. [CrossRef]
6. Fisher, H.; Drummond, A. A call to arms: The emergency physician, international perspectives on firearm injury prevention and the canadian gun control debate. *J. Emerg. Med.* **1999**, *17*, 529–537. [CrossRef]
7. Jain, S.K.; Singh, B.P.; Singh, R.P. Indian homemade firearm—A technical review. *Forensic Sci. Int.* **2004**, *144*, 11–18. [CrossRef]
8. Adams, R.J. Retailer–manufacturer responsibility in the marketing of firearms: Exploring the concept of negligent distribution. *J. Retail. Consum. Serv.* **2004**, *11*, 161–169. [CrossRef]
9. Breeze, J.; Cooper, H.; Pearson, C.R.; Henney, S.; Reid, A. Ear injuries sustained by British service personnel subjected to blast trauma. *J. Laryngol. Otol.* **2011**, *125*, 13–17. [CrossRef]
10. Guida, H.L.; Diniz, T.H.; Kinoshita, S.K. Acoustic and psychoacoustic analysis of the noise produced by the police force firearms. *Braz. J. Otorhinolaryngol.* **2011**, *77*, 163–170. [CrossRef]
11. Junuzovic, M.; Midlöv, P.; Lönn, S.L.; Eriksson, A. Swedish hunters' safety behaviour and experience of firearm incidents. *Accid. Anal. Prev.* **2013**, *60*, 64–70. [CrossRef]

12. Jones, H.G.; Greene, N.T.; Ahroon, W.A. Human middle-ear muscles rarely contract in anticipation of acoustic impulses: Implications for hearing risk assessments. *Hear. Res.* **2019**, *378*, 53–62. [CrossRef] [PubMed]
13. Chau, J.K.; Cho, J.J.W.; Fritz, D.K. Evidence-Based Practice. *Otolaryngol. Clin. N. Am.* **2012**, *45*, 941–958. [CrossRef] [PubMed]
14. Guida, H.L.; Taxini, C.L.; de Oliveira Gonçalves, C.G.; Valenti, V.E. Evaluation of hearing protection used by police officers in the shooting range. *Braz. J. Otorhinolaryngol.* **2014**, *80*, 515–521. [CrossRef] [PubMed]
15. Yankaskas, K. Prelude: Noise-induced tinnitus and hearing loss in the military. *Hear. Res.* **2013**, *295*, 3–8. [CrossRef]
16. Kim, D.; Cheong, C.; Jeong, W.B. The use of a hybrid model to compute the nonlinear acoustic performance of silencers for the finite amplitude acoustic wave. *J. Sound Vib.* **2010**, *329*, 2158–2176. [CrossRef]
17. Lou, G.; Wu, T.W.; Cheng, C.Y.R. Boundary element analysis of packed silencers with a substructuring technique. *Eng. Anal. Bound. Elem.* **2003**, *27*, 643–653. [CrossRef]
18. Kirby, R.; Amott, K.; Williams, P.T.; Duan, W. On the acoustic performance of rectangular splitter silencers in the presence of mean flow. *J. Sound Vib.* **2014**, *333*, 6295–6311. [CrossRef]
19. Bilawchuk, S.; Fyfe, K.R. Comparison and implementation of the various numerical methods used for calculating transmission loss in silencer systems. *Appl. Acoust.* **2003**, *64*, 903–916. [CrossRef]
20. Ming Wong, L.; Gary Wang, G. Development of an automatic design and optimization system for industrial silencers. *J. Manuf. Syst.* **2003**, *22*, 327–339. [CrossRef]
21. Pollak, S.; Saukko, P. Gunshot Wounds. In *Encyclopedia of Forensic Sciences*; Elsevier: Amsterdam, The Netherlands, 2013; pp. 70–82, ISBN 978-0-12-382166-9.
22. Haag, M.G.; Haag, L.C. Sound Levels of Gunshots, Supersonic Bullets, and Other Impulse Sounds. In *Shooting Incident Reconstruction*; Elsevier: Amsterdam, The Netherlands, 2011; pp. 295–329, ISBN 978-0-12-382241-3.
23. Davis, R.R.; Clavier, O. Impulsive noise: A brief review. *Hear. Res.* **2017**, *349*, 34–36. [CrossRef]
24. Miller, M.T. Crime Scene Reconstruction. In *Crime Scene Investigation Laboratory Manual*; Elsevier: Amsterdam, The Netherlands, 2018; pp. 191–200, ISBN 978-0-12-812845-9.
25. Pääkkönen, R.; Anttonen, H.; Niskanen, J. Noise control on military shooting ranges for rifles. *Appl. Acoust.* **1991**, *32*, 49–60. [CrossRef]
26. Meng, X.; Wang, Z.; Zhang, Z.; Wang, F. A Method for Monitoring the Underground Mining Position Based on the Blasting Source Location. *Meas. Sci. Rev.* **2013**, *13*, 45–49. [CrossRef]
27. Hristov, N.; Kari, A.; Jerković, D.; Savić, S.; Sirovatka, R. Simulation and Measurements of Small Arms Blast Wave Overpressure in the Process of Designing a Silencer. *Meas. Sci. Rev.* **2015**, *15*, 27–34. [CrossRef]
28. Sallai, J.; Hedgecock, W.; Volgyesi, P.; Nadas, A.; Balogh, G.; Ledeczi, A. Weapon classification and shooter localization using distributed multichannel acoustic sensors. *J. Syst. Archit.* **2011**, *57*, 869–885. [CrossRef]
29. Vogel, H.; Dootz, B. Wounds and weapons. *Eur. J. Radiol.* **2007**, *63*, 151–166. [CrossRef]
30. Brożek-Mucha, Z. A study of gunshot residue distribution for close-range shots with a silenced gun using optical and scanning electron microscopy, X-ray microanalysis and infrared spectroscopy. *Sci. Justice* **2017**, *57*, 87–94. [CrossRef]
31. Monturo, C. Ammunition. In *Forensic Firearm Examination*; Elsevier: Amsterdam, The Netherlands, 2019; pp. 21–71, ISBN 978-0-12-814539-5.
32. Liu, N.; Alexander, A.A.; Li, X.; Wang, S.; Lu, W.F.; Sulaimee, N.H.B.; Chew, C.-M. Modelling of abrasive blasting process from viewpoint of energy exchange. In Proceedings of the 2018 IEEE 23rd International Conference on Emerging Technologies and Factory Automation (ETFA), Turin, Italy, 4–7 September 2018; pp. 488–492.
33. Carson, R.A.; Sahni, O. Scaling Laws for the Peak Overpressure of a Cannon Blast. *J. Fluids Eng.* **2016**, *139*, 021204. [CrossRef]
34. Kong, B.; Lee, K.; Park, S.-R.; Jang, S.; Lee, S. Prediction of sound field from recoilless rifles in terms of source decomposition. *Appl. Acoust.* **2015**, *88*, 137–145. [CrossRef]
35. Costa, E.; Lagasco, F. Development of a 3D numerical methodology for fast prediction of gun blast induced loading. *Shock Waves* **2014**, *24*, 257–265. [CrossRef]
36. Cummings, A. High Frequency Ray Acoustics Models for Duct Silencers. *J. Sound Vib.* **1999**, *221*, 681–708. [CrossRef]
37. Fang, Z.; Liu, C.Y. Semi-weak-form mesh-free method for acoustic attenuation analysis of silencers with arbitrary but axially uniform transversal sections. *J. Sound Vib.* **2019**, *442*, 752–769. [CrossRef]

38. Kilikevicius, A.; Skeivalas, J.; Jurevicius, M.; Turla, V.; Kilikeviciene, K.; Bureika, G.; Jakstas, A. Experimental investigation of dynamic impact of firearm with suppressor. *Indian J. Phys.* **2017**, *91*, 1077–1087. [CrossRef]
39. Lu, Y.; Zhou, K.; He, L.; Li, J.; Huang, X. Research on the floating performance of a novel large caliber machine gun based on the floating principle with complicated boundary conditions. *Def. Technol.* **2019**, *15*, 607–614. [CrossRef]
40. Libal, U.; Spyra, K. Wavelet based shock wave and muzzle blast classification for different supersonic projectiles. *Expert Syst. Appl.* **2014**, *41*, 5097–5104. [CrossRef]
41. Carson, R.A.; Sahni, O. Study of the relevant geometric parameters of the channel leak method for blast overpressure attenuation for a large caliber cannon. *Comput. Fluids* **2015**, *115*, 211–225. [CrossRef]
42. Mäkinen, T.; Pertilä, P. Shooter localization and bullet trajectory, caliber, and speed estimation based on detected firing sounds. *Appl. Acoust.* **2010**, *71*, 902–913. [CrossRef]
43. Qin, Q.; Zhang, X. Numerical investigation on combustion in muzzle flows using an inert gas labeling method. *Int. J. Heat Mass Transf.* **2016**, *101*, 91–103. [CrossRef]
44. Guo, Z.X.; Pan, Y.T.; Li, K.W.; Zhang, H.Y. Numerical Simulation of Overpressure about Muzzle Blast Flowfield. *Adv. Mater. Res.* **2012**, *605–607*, 2506–2509. [CrossRef]
45. Xiao, W.; Andrae, M.; Gebbeken, N. Experimental and numerical investigations on the shock wave attenuation performance of blast walls with a canopy on top. *Int. J. Impact Eng.* **2019**, *131*, 123–139. [CrossRef]
46. Mouritz, A.P. Advances in understanding the response of fibre-based polymer composites to shock waves and explosive blasts. *Compos. Part A Appl. Sci. Manuf.* **2019**, *125*, 105502. [CrossRef]
47. Hu, X.-D.; Zhao, G.-F.; Deng, X.-F.; Hao, Y.-F.; Fan, L.-F.; Ma, G.-W.; Zhao, J. Application of the four-dimensional lattice spring model for blasting wave propagation around the underground rock cavern. *Tunn. Undergr. Space Technol.* **2018**, *82*, 135–147. [CrossRef]
48. Lu, G.; Fall, M. Modelling blast wave propagation in a subsurfacegeotechnical structure made of an evolutive porous material. *Mech. Mater.* **2017**, *108*, 21–39. [CrossRef]
49. Carson, R.A.; Sahni, O. Numerical Investigation of Channel Leak Geometry for Blast Overpressure Attenuation in a Muzzle Loaded Large Caliber Cannon. *J. Fluids Eng.* **2014**, *137*, 021102. [CrossRef]
50. Lee, H.-S.; Kang, T.-Y.; Hong, J.-H. Development of a Muffler for 40 mm Medium Caliber Gun: Numerical Analysis and Validation. *Int. J. Precis. Eng. Manuf.* **2018**, *19*, 245–250. [CrossRef]
51. Yuanjuan, Z. Study on Attenuation Law of Open-pit Bench Blasting Vibration. *Procedia Eng.* **2014**, *84*, 868–872. [CrossRef]
52. Lee, J.S.; Ahn, S.K.; Sagong, M. Attenuation of blast vibration in tunneling using a pre-cut discontinuity. *Tunn. Undergr. Space Technol.* **2016**, *52*, 30–37. [CrossRef]
53. Sugiyama, Y.; Homae, T.; Wakabayashi, K.; Matsumura, T.; Nakayama, Y. Numerical simulations on the attenuation effect of a barrier material on a blast wave. *J. Loss Prev. Process Ind.* **2014**, *32*, 135–143. [CrossRef]
54. Wierschem, N.E.; Hubbard, S.A.; Luo, J.; Fahnestock, L.A.; Spencer, B.F.; McFarland, D.M.; Quinn, D.D.; Vakakis, A.F.; Bergman, L.A. Response attenuation in a large-scale structure subjected to blast excitation utilizing a system of essentially nonlinear vibration absorbers. *J. Sound Vib.* **2017**, *389*, 52–72. [CrossRef]
55. Igra, O.; Falcovitz, J.; Houas, L.; Jourdan, G. Review of methods to attenuate shock/blast waves. *Prog. Aerosp. Sci.* **2013**, *58*, 1–35. [CrossRef]
56. Girin, A. Attenuation of a point blast shock wave in the dusty air. *J. Loss Prev. Process Ind.* **2013**, *26*, 1569–1573. [CrossRef]
57. Huang, Z.; Wessam, M.E.; Chen, Z. Numerical investigation of the three-dimensional dynamic process of sabot discard. *J. Mech. Sci. Technol.* **2014**, *28*, 2637–2649. [CrossRef]
58. Carson, R.A.; Sahni, O. Numerical investigation of propellant leak methods in large-caliber cannons for blast overpressure attenuation. *Shock Waves* **2014**, *24*, 625–638. [CrossRef]
59. Kang, K.-J.; Ko, S.-H.; Lee, D.-S. A study on impulsive sound attenuation for a high-pressure blast flowfield. *J. Mech. Sci. Technol.* **2008**, *22*, 190–200. [CrossRef]
60. Rehman, H.; Chung, H.; Joung, T.; Suwono, A.; Jeong, H. CFD analysis of sound pressure in tank gun muzzle silencer. *J. Cent. South Univ. Technol.* **2011**, *18*, 2015–2020. [CrossRef]
61. Scaling of Air Blast Waves. In *Fundamental Studies in Engineering*; Elsevier: Amsterdam, The Netherlands, 1991; Volume 12, pp. 49–69, ISBN 978-0-444-88156-4.
62. Explosions and Pressure Waves. In *Industrial Safety Series*; Elsevier: Amsterdam, The Netherlands, 1994; Volume 3, pp. 445–462, ISBN 978-0-444-89863-0.

63. Krehl, P. History of Shock Waves. In *Handbook of Shock Waves*; Elsevier: Amsterdam, The Netherlands, 2001; pp. 1–142, ISBN 978-0-12-086430-0.
64. Phadnis, V.A.; Silberschmidt, V.V. 8.14 Composites Under Dynamic Loads at High Velocities. In *Comprehensive Composite Materials II*; Elsevier: Amsterdam, The Netherlands, 2018; pp. 262–285, ISBN 978-0-08-100534-7.
65. Phadnis, V.A.; Roy, A.; Silberschmidt, V.V. Dynamic damage in FRPs. In *Dynamic Deformation, Damage and Fracture in Composite Materials and Structures*; Elsevier: Amsterdam, The Netherlands, 2016; pp. 193–222, ISBN 978-0-08-100870-6.
66. Guo, Z. Numerical Simulation of Muzzle Blast Overpressure in Antiaircraft Gun Muzzle Brake. *J. Inf. Comput. Sci.* **2013**, *10*, 3013–3019. [CrossRef]
67. Cheng, L.; Ji, C.; Zhong, M.; Long, Y.; Gao, F. Full-scale experimental investigation on the shock-wave characteristics of high-pressure natural gas pipeline physical explosions. *Int. J. Hydrog. Energy* **2019**, *44*, 20587–20597. [CrossRef]
68. Fang, B.; Wang, Y.-G.; Zhao, Q. On multi-dimensional linear stability of planar shock waves for Chaplygin gases. *Appl. Math. Lett.* **2020**, *102*, 106085. [CrossRef]
69. Yazdandoost, F.; Sadeghi, O.; Bakhtiari-Nejad, M.; Elnahhas, A.; Shahab, S.; Mirzaeifar, R. Energy dissipation of shock-generated stress waves through phase transformation and plastic deformation in NiTi alloys. *Mech. Mater.* **2019**, *137*, 103090. [CrossRef]
70. Hokamoto, K.; Fujita, M. Shock-wave research on condensed matter at the High-Energy Rate Laboratory of Kumamoto University—An introduction. *Phys. B Condens. Matter* **1997**, *239*, 187–190. [CrossRef]
71. Wu, J.; Liu, X.; Zhao, J.; Qiao, H.; Zhang, Y.; Zhang, H. The online monitoring method research of laser shock processing based on plasma acoustic wave signal energy. *Optik* **2019**, *183*, 1151–1159. [CrossRef]
72. Otsuka, F.; Matsukiyo, S.; Hada, T. PIC Simulation of a quasi-parallel collisionless shock: Interaction between upstream waves and backstreaming ions. *High Energy Density Phys.* **2019**, *33*, 100709. [CrossRef]
73. Xu, H.; Gao, J.; Yao, A.; Yao, C. The relief of energy convergence of shock waves by using the concave combustion chamber under severe knock. *Energy Convers. Manag.* **2018**, *162*, 293–306. [CrossRef]
74. Tonicello, N.; Lodato, G.; Vervisch, L. Entropy preserving low dissipative shock capturing with wave-characteristic based sensor for high-order methods. *Comput. Fluids* **2020**, *197*, 104357. [CrossRef]
75. Kirby, R. Simplified Techniques for Predicting the Transmission Loss of A Circular Dissipative Silencer. *J. Sound Vib.* **2001**, *243*, 403–426. [CrossRef]
76. Wei, Z.; Weavers, L.K. Combining COMSOL modeling with acoustic pressure maps to design sono-reactors. *Ultrason. Sonochem.* **2016**, *31*, 490–498. [CrossRef]
77. Carlucci, D.E.; Decker, R.; Vega, J.; Ray, D. Measurement of in-bore side loads and comparison to first maximum yaw. *Def. Technol.* **2016**, *12*, 106–112. [CrossRef]
78. Courtney, E.; Couvillion, R.; Courtney, A.; Courtney, M. Effects of Sound Suppressors on Muzzle Velocity, Bullet Yaw and Drag. In Proceedings of the 30th International Symposium on Ballistics, Long Beach, CA, USA, 11–15 September 2017; DEStech Publications, Inc.: Lancaster, Pennsylvania, 2017.
79. Lobarinas, E.; Scott, R.; Spankovich, C.; Le Prell, C.G. Differential effects of suppressors on hazardous sound pressure levels generated by AR-15 rifles: Considerations for recreational shooters, law enforcement, and the military. *Int. J. Audiol.* **2016**, *55*, S59–S71. [CrossRef]
80. Lankford, J.E.; Meinke, D.K.; Flamme, G.A.; Finan, D.S.; Stewart, M.; Tasko, S.; Murphy, W.J. Auditory risk of air rifles. *Int. J. Audiol.* **2016**, *55*, S51–S58. [CrossRef]
81. Meinke, D.K.; Murphy, W.J.; Finan, D.S.; Lankford, J.E.; Flamme, G.A.; Stewart, M.; Soendergaard, J.; Jerome, T.W. Auditory risk estimates for youth target shooting. *Int. J. Audiol.* **2014**, *53*, S16–S25. [CrossRef]
82. Mlynski, R.; Kozlowski, E. Selection of Level-Dependent Hearing Protectors for Use in An Indoor Shooting Range. *Int. J. Environ. Res. Public Health* **2019**, *16*, 2266. [CrossRef]
83. Murphy, W.J.; Tasko, S.M.; Finan, D.; Meinke, D.K.; Stewart, M.; Lankford, J.E.; Campbell, A.R.; Flamme, G. Referee whistles Part II—Outdoor sound power assessment. *J. Acoust. Soc. Am.* **2019**, *145*, 1816. [CrossRef]
84. Skrodzka, E.; Wicher, A.; Gołębiewski, R. A Review of Gunshot Noise as Factor in Hearing Disorders. *Acta Acust. United Acust.* **2019**, *105*, 904–911. [CrossRef]
85. Stewart, M. What to Know about Firearm Suppressors and Hearing Loss: Does a firearm suppressor always do enough to protect hearing? No. Should firearm users also wear hearing protection? Yes. *ASHA Lead.* **2018**, *23*, 18–20. [CrossRef]

86. Murphy, W.J.; Campbell, A.R.; Flamme, G.A.; Tasko, S.M.; Lankford, J.E.; Meinke, D.K.; Finan, D.S.; Stewart, M.; Zechmann, E.L. Developing a method to assess noise reduction of firearm suppressors for small-caliber weapons. *Proc. Meet. Acoust.* **2018**, *33*, 040004.
87. Murphy, W.J.; Campbell, A.R.; Flamme, G.A.; Tasko, S.M.; Lankford, J.E.; Meinke, D.K.; Finan, D.S.; Zechmann, E.L.; Stewart, M. The attenuation of firearm suppressors as a function of angle and bullet velocity. In Proceedings of the National Hearing Conservation Association, Orlando, FL, USA, 15–17 February 2018.
88. Murphy, W.J.; Flamme, G.A.; Campbell, A.R.; Zechmann, E.L.; Tasko, S.M.; Lankford, J.E.; Meinke, D.K.; Finan, D.S.; Stewart, M. The reduction of gunshot noise and auditory risk through the use of firearm suppressors and low-velocity ammunition. *Int. J. Audiol.* **2018**, *57*, S28–S41. [CrossRef]
89. Yue, B.; Guddati, M.N. Dispersion-reducing finite elements for transient acoustics. *J. Acoust. Soc. Am.* **2005**, *118*, 2132–2141. [CrossRef]
90. Kilikevičienė, K.; Matijošius, J.; Fursenko, A.; Kilikevičius, A. Tests of hail simulation and research of the resulting impact on the structural reliability of solar cells. *Ekspolatacja Niezawodn. Maint. Reliab.* **2019**, *21*, 275–281. [CrossRef]
91. Kilikevičius, A.; Skeivalas, J.; Kilikevičienė, K.; Matijošius, J. Analysis of Dynamic Parameters of a Railway Bridge. *Appl. Sci.* **2019**, *9*, 2545. [CrossRef]